Design and Construction of a Cyclotron
Capable of Accelerating Protons to 2 MeV

by

Leslie Dewan

Submitted to the Department of Nuclear Science and Engineering
in Partial Fulfillment of the Requirements for the Degree of

Bachelor of Science in Nuclear Science and Engineering
at the
Massachusetts Institute of Technology

June 2007

Signature of Author: _____

Leslie Dewan
Department of Nuclear Science and Engineering
May 16, 2007

Certified by: _____

David G. Cory
Professor of Nuclear Science and Engineering
Thesis Supervisor

Accepted by: _____

David G. Cory
Professor of Nuclear Science and Engineering
Chairman, NSE Committee for Undergraduate Students

Design and Construction of a Cyclotron
Capable of Accelerating Protons to 2 MeV

by

Leslie Dewan

Submitted to the Department of Nuclear Science and Engineering on May 16, 2007
in Partial Fulfillment of the Requirements for the Degree of
Bachelor of Science in Nuclear Science and Engineering

ABSTRACT

This thesis describes the design and construction of a cyclotron capable of accelerating protons to 2 MeV. A cyclotron is a charged particle accelerator that uses a magnetic field to confine particles to a spiral flight path in a vacuum chamber. An applied electrical field accelerates these particles to high energies, typically on the order of mega-electron volts. This cyclotron can be used by students in the Department of Nuclear Engineering to perform experiments with low energy proton beams. For example, this cyclotron could be used for experiments involving the Li7(p,n)Be7 reaction, which requires protons with energies on the order of 2 MeV [2].

Thesis Supervisor: David G. Cory
Title: Professor of Nuclear Science and Engineering

Contents

List of Figures

Introduction

A cyclotron is a charged particle accelerator that uses a magnetic field to confine particles to a spiral flight path in a vacuum chamber. An applied electrical field accelerates these particles to high energies, typically on the order of mega-electron volts. Figure 1 shows the vacuum chamber and electrodes of an early cyclotron, built by Ernest Lawrence and Stanley Livingston in 1931.

A particle in a cyclotron encounters the same accelerating electric field many times along its spiral flight path. This flight path is shown schematically in Figure 2. Using the accelerating field in this fashion allows a cyclotron to produce high-energy particles far more efficiently than other accelerators, such as linear accelerators.

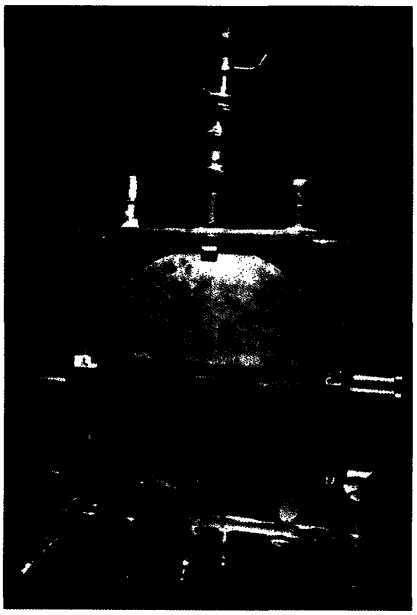

Figure 1. Cyclotron built by E. Lawrence and S. Livingston in 1931. (from the National Museum of Science and Industry, UK)

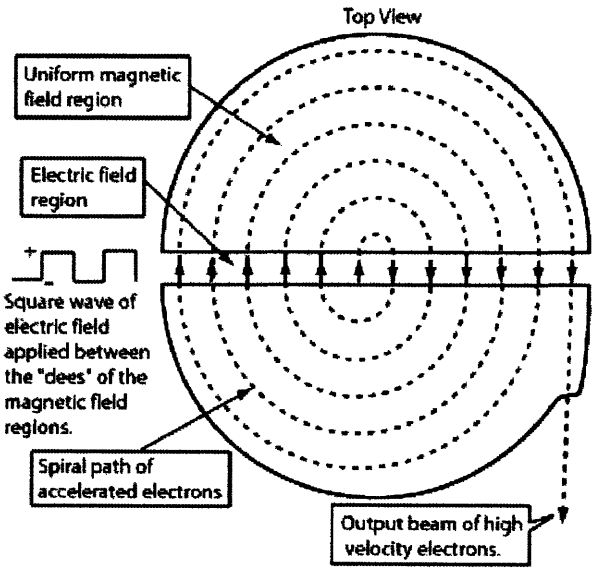

Figure 2. Schematic showing particles' flight path in a cyclotron, as well as the applied magnetic and electric fields. (from Georgia State University)

The force of the magnetic field on the charged particles is described by the following relation:

$$F = qvB = \frac{mv^2}{r} \quad (1)$$

where B is the magnetic field in Tesla, r is the particle's radius in meters, m is the particle's mass in kg, and q is the particle's charge in Coulombs. This equation can be rearranged to give the particle's velocity as a function of the other variables:

$$v = \frac{qBr}{m} \quad (2)$$

This velocity can be used to derive the angular frequency of the particle's flight path.

$$f = \frac{v}{2\pi r} = \frac{qBr}{m}\frac{1}{2\pi r} = \frac{qB}{2\pi m} \quad (3)$$

The signal applied to the cyclotron's electrodes must oscillate at this frequency. The particles' maximum kinetic energy can also be determined from equation 2:

$$KE = \frac{1}{2}\frac{mv^2}{r} = \frac{1}{2}\frac{mq^2B^2r^2}{m^2} = \frac{q^2B^2r^2}{2m} \quad (4a)$$

As shown in equation 4a, the particles' maximum energy depends on the strength of the magnetic field. A larger magnetic field exerts a greater centripetal force on the particles (by equation 1), making their flight path a tighter spiral. A particle traveling along this tighter spiral encounters the electrical field more often, and is therefore accelerated to a greater velocity and kinetic energy.

Thesis Objectives

The purpose of this thesis is to design and construct a cyclotron capable of accelerating protons to 2 MeV. This cyclotron can be used by students in the Department of Nuclear Engineering to perform experiments with low energy proton beams. For example, this cyclotron could be used for experiments involving the Li6(p,n)Be7 reaction, which requires protons with energies on the order of 2 MeV [2].

Preliminary Analysis and Research

Some preliminary analysis was necessary before starting to design the cyclotron's components. Specifically, this analysis determined the type of charged particles to accelerate and the range of energies to which these particles could be accelerated. The particles' maximum energy determines the types of reactions they can undergo.

There are certain difficulties inherent in accelerating electrons to high velocities. Electrons are approximately 1800 times less massive than protons. By equation 2, a system with a given magnetic field strength and radius would be able to accelerate electrons to velocities 1800 times greater than the maximum proton velocity, neglecting relativistic effects. Charged particles moving along a curved flight path at high velocities emit high-energy photons, which must be shielded. In this cyclotron, which has a maximum magnetic field strength of approximately 2.5 Tesla and radius of approximately 8 cm, protons are not able to reach a high enough velocity to emit this radiation. However, accelerated electrons would emit photons with energies in the x-ray range. It was decided to accelerate protons in this cyclotron because the system would not require extensive shielding. It is also straightforward to generate protons by ionizing hydrogen.

As shown in equations 1, 2, and 3, and 4a the protons' maximum attainable energy is limited by the dimensions of the magnet's poles and its maximum field strength. The magnetic field strength is a function of the separation distance between the north and south poles of the electromagnet. This cyclotron's magnetic field is produced using a Varian V-3900 magnet. Figure 3 shows the relation between gap distance and magnetic field intensity for this magnet.

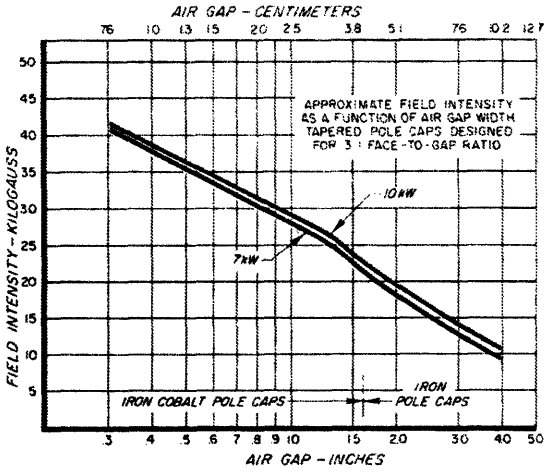

Figure 3. Magnetic field intensity as a function of gap distance for a Varian V-3900 magnet (from Varian Analytical Instrument Division V-3900 manual).

As shown in Figure 3, the magnet generates 2.7 T of magnetic field with a 1.25 inch pole separation. By equations 4b and 5, protons accelerated through a vacuum while contained in this magnetic field can attain a maximum energy of approximately 2 MeV.

$$KE = \frac{1}{2}\frac{mv^2}{r} = \frac{1}{2}\frac{mq^2B^2r^2}{m^2} = \frac{q^2B^2r^2}{2m} = \frac{(1.6\cdot10^{-19})^2(2.7)^2(0.075)^2}{2\cdot1.67\cdot10^{-27}} = 3.143\text{E-}13\ \text{J} \qquad (4b)$$

$$3.143\cdot10^{-13}J\frac{1\,MeV}{1.6\cdot10^{-13}J} = 1.96\ \text{MeV} \qquad (5)$$

This maximum proton energy determines the reactions that the protons could undergo with a target. These protons have a sufficiently high kinetic energy to undergo the Li7(p,n)Be7 reaction. As shown in Figure 4, this reaction requires particles with energies of at least 1.882 MeV.

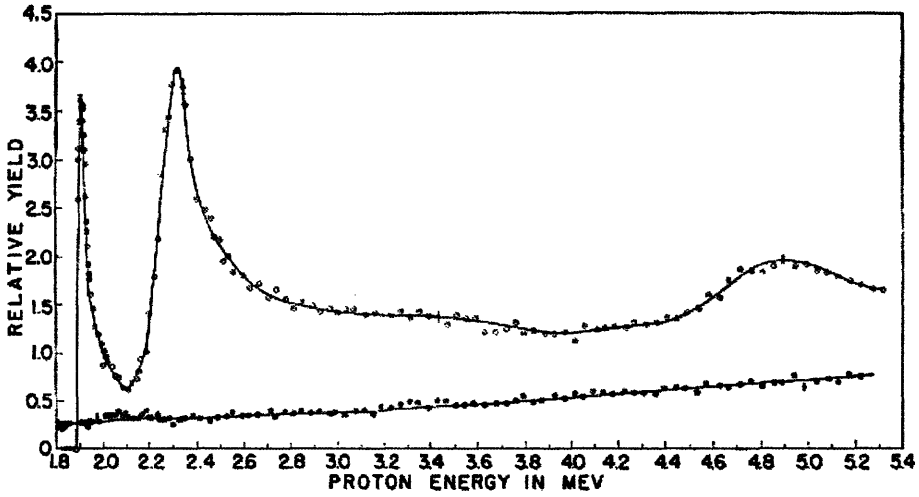

Figure 4. Yields from the proton bombardment of lithium. The uppermost curve represents relative neutron yields. The threshold of the Li7(p,n)Be7 reaction is at 1.882 MeV. (Bair 1952)

It is possible to accelerate protons to this energy with the existing pole pieces in place. The existing pole pieces have an 8 cm radius and a separation gap of 1.25 inches. By equations (4b) and (5), this geometry and field strength is capable of accelerating protons to a maximum kinetic energy of 1.96 MeV. It is possible to acquire lower energy particles by positioning the detector at a smaller radius. A detector positioned 7.34 centimeters from the center of the accelerator will intercept particles with energies of approximately 1.88 MeV in the presence of a 2.7 T magnetic field.

The presence of this strong magnetic field means that all cyclotron components must be made of magnetically transparent materials such as aluminum, copper, or brass. The magnetic field would cause oscillations, which would disrupt measurements, in materials such as steel that are not magnetically transparent.

Vacuum Chamber

Determining Required Vacuum Pressure

The MATLAB simulation shown in Appendix A calculates the protons' flight distance as a function of the magnetic field strength. It also plots the protons' mean free path as a function of the vacuum pressure inside the chamber. The mean free path of a particle is the average distance a

particle travels between collisions. For a particle moving at a high velocity compared to a set of target particles, the mean free path is given by equation 6.

$$l=(n\sigma)^{-1} \tag{6}$$

where l is the mean free path, n is the number of particles per unit volume, and sigma is the target particles' cross-sectional area. The number of particles per unit volume depends on the pressure inside the vacuum chamber by the ideal gas law.

$$n=\frac{P}{kT} \tag{7}$$

where P is the pressure in Pascals, T is the temperature in Kelvin, and k is Boltzmann's constant, which is equal to 1.38066 x 10^{-23} J/K.

An acceptable vacuum would allow for a mean free path an order of magnitude larger than the expected flight distance. For protons accelerated by a 2.7 T magnetic field and a voltage difference of 1000 V between the electrodes, the expected flight distance is approximately 300 meters. Figure 5 is a graph of the particle's mean free path versus the degree of vacuum, in Torr, in which they are traveling.

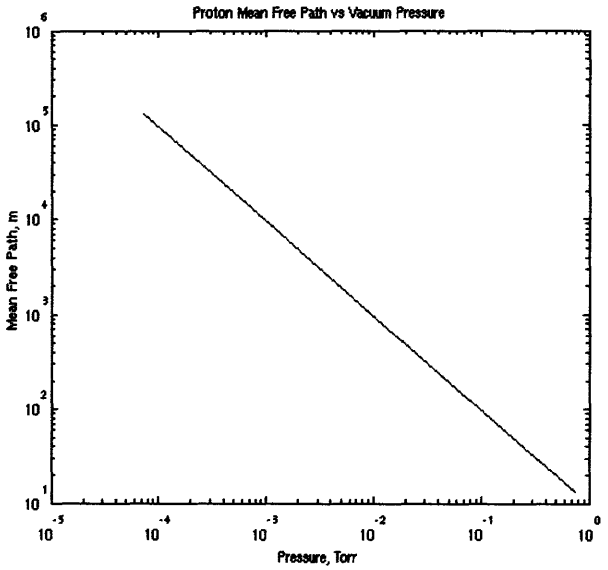

Figure 5. Proton mean free path in meters versus vacuum pressure in Torr.

Testing the Vacuum Chamber

The vacuum chamber was pumped using a Varian Turbo-V 70 vacuum pump. The vacuum chamber can be consistently pumped down to approximately $2*10^{-3}$ Torr. According to Figure 5, this corresponds to a mean free path of 5 kilometers, which is approximately an order of magnitude longer than the protons' expected path length.

Vacuum Chamber Ports

The vacuum chamber contains the two copper electrodes used to accelerate the protons, and an ion source. This chamber has a series of ports, which connect it to (1) a signal generator and RF matching box; (2) a vacuum pump that maintains low pressure in the chamber; (3) filament leads for the ion source; (4) a hydrogen supply for the ion source; and (5) a target to collect the accelerated particles. Figure 6 shows the position of these five ports on the vacuum chamber.

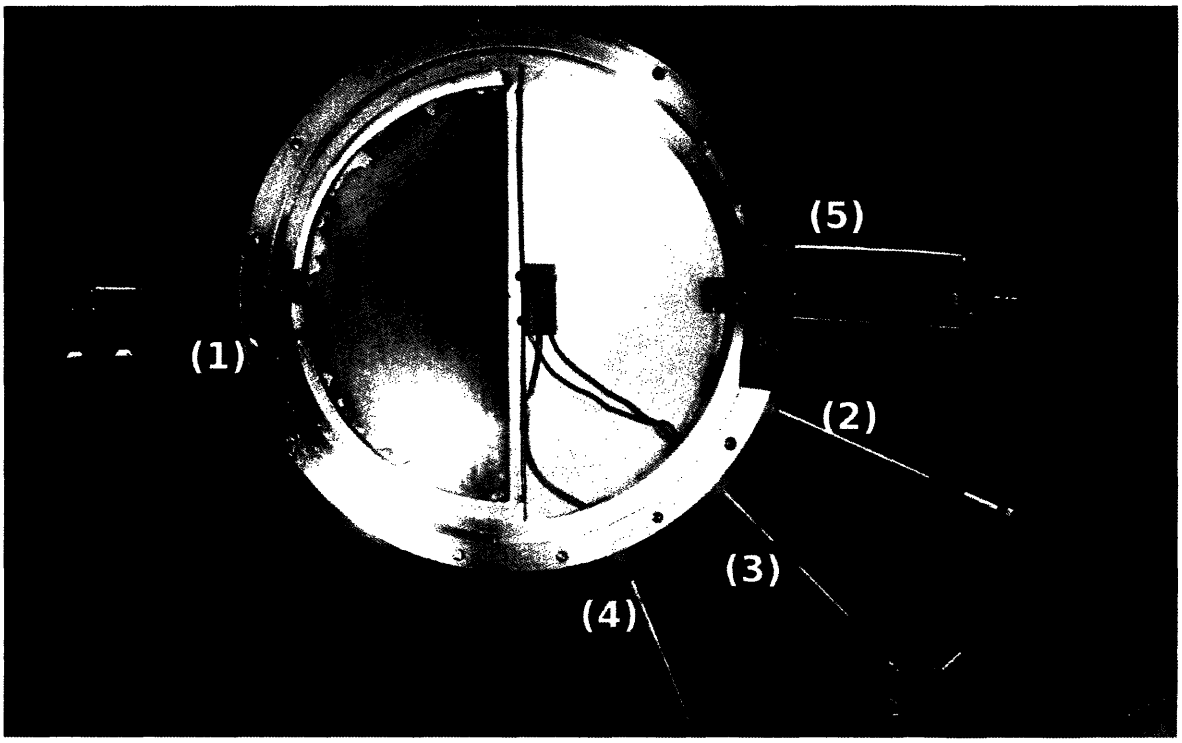

Figure 6. Vacuum chamber and numbered ports, connecting to the following subsystems: (1) RF system; (2) vacuum pump to maintain low pressure in the chamber; (3) filament leads for the ion source; (4) a hydrogen supply for the ion source; and (5) a target to collect the accelerated particles.

Details of Design and Construction

The sides of the vacuum chamber are made of 6061 aluminum. The vacuum chamber lids are made of 7075 aluminum, because that alloy has a significantly larger tensile strength and yield strength than 6061 aluminum, as shown in Table 2.

Table 2. Properties of Aluminum Alloys (from Machinery's Handbook).

Alloy	Young's Modulus (GPa)	Yield Strength (MPa)
6061-T6	69	275
7075-T6	75	505

The chamber lids are subject to significant stresses because of the low pressure inside the chamber. Following equation 8, which describes the deflection of a circular plate under uniform load with a fixed support around the entire outer boundary, a lid with radius 10 centimeters and thickness of 3.5 millimeters would undergo less than 1 mm of deflection when covering a chamber with internal pressure of 10^{-3} Torr. These calculations were also verified experimentally—pumping the chamber to vacuum resulted in no visible lid deflection.

$$\delta_{center}=\frac{-qa^4}{2D}(L_{14}-L_{11}) \tag{8a}$$

$$D=\frac{Et^3}{12(1-\nu^2)} \tag{8b}$$

$$L_{11}=\frac{1}{64}(1+4(\frac{r_0}{a})^2-5(\frac{r_0}{a})^4-4(\frac{r_0}{a})^2(2+(\frac{r_0}{a})^2)\ln(\frac{a}{r_0})) \tag{8c}$$

$$L_{14}=\frac{1}{16}(1-(\frac{r_0}{a})^4-4(\frac{r_0}{a})^2)\ln(\frac{a}{r_0}) \tag{8d}$$

In equation 8, a is the plate radius in meters, r_0 is the outermost radius at which the distributed load is applied q is the linearized load in Newtons per meter, t is the plate thickness in millimeters, E is the modulus of elasticity and v is the Poisson ratio.

The chamber has two grooves for Viton o-rings, which make the connection between the side and lids vacuum-tight. The chamber's ports were made by screwing lengths of pipe, which were sealed with Teflon tape, into tapped holes in the side of the chamber. The other ends of the pipes were screwed onto QF flanges.

Electrodes

Principles of operation

Smaller cyclotrons often accelerate particles using two dee-shaped electrodes. Figure 1 shows an example of this design. This cyclotron uses an alternative design: it has one dee-shaped copper electrode, and the grounded vacuum chamber functions as the other electrode. Figure 7 shows the shape and positioning of the electrode with respect to the vacuum chamber.

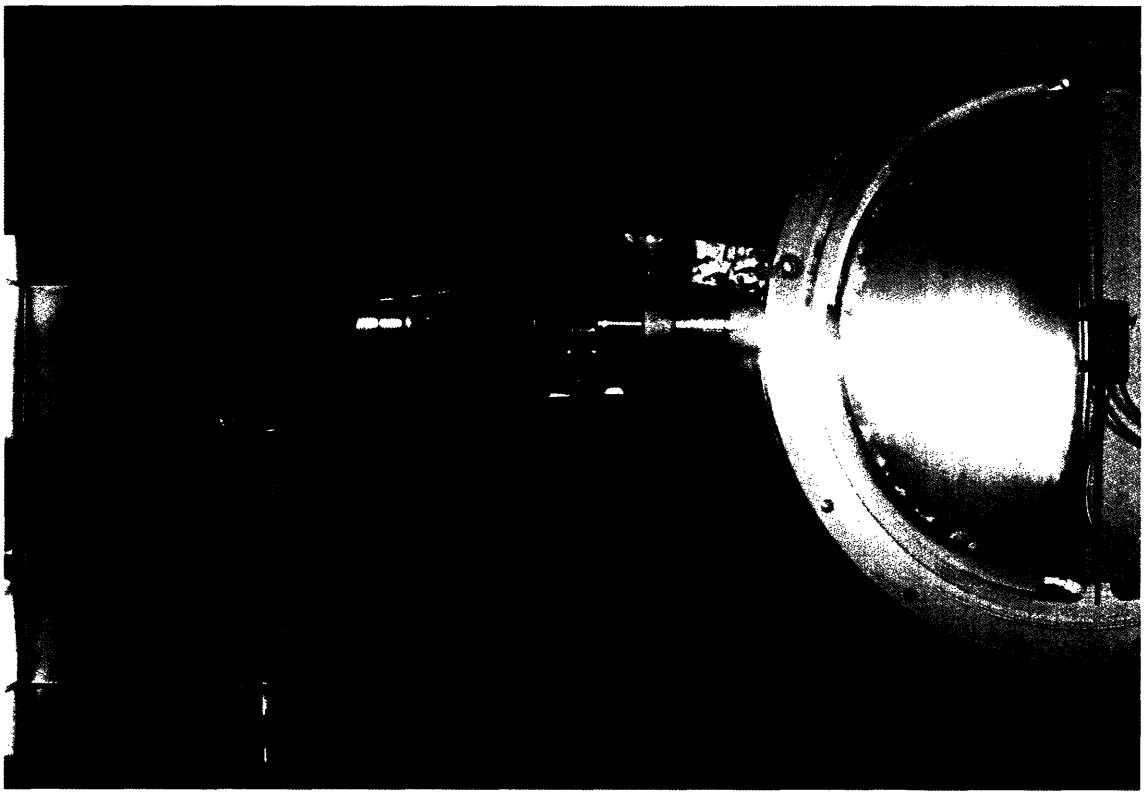

Figure 7. Copper electrodes and connection to RF system, with copper grounding strap to ensure consistent connection to ground.

Details of Construction

The dee-shaped electrode was made by first cutting pieces of copper on an OMAX waterjet machine, then soldering the pieces together. A length of copper rod was then soldered to the dee. The copper rod was threaded at one end to make an electrical connection with an RF feedthrough (Varian Vacuum, part number 9545143). The feedthrough connects to the RF control box, as shown in Figure 7.

RF system

Principles of Design

The RF system ensures that the cyclotron's impedance is matched with the incoming signal impedance, which is 50 Ohms. An impedance mismatch would cause a fraction of the incident power to be reflected, making the system less efficient. The cyclotron electrodes and vacuum chamber act as a capacitor. This capacitor in parallel with an inductor resonates at a particular frequency, given by equation 9.

$$f = \frac{1}{2\pi\sqrt{LC}} \tag{9}$$

Placing an additional variable capacitor in series with the system makes it possible to tune the system's impedance to 50 Ohms. Figure 8 is a circuit diagram of the resonator and tuning capacitor.

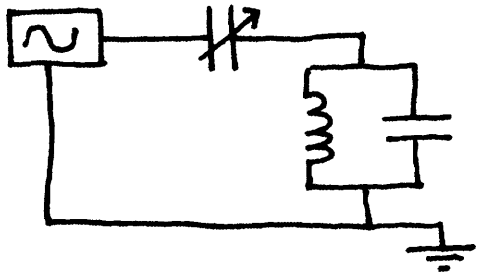

Figure 8. Schematic of resonator and tuning capacitor.

Tuning and testing the RF system

First, the capacitance in vacuum chamber was determined by placing a coil with an arbitrary inductance in series with the cyclotron chamber, and measuring the resonant frequency with the network analyzer. Next, the same arbitrary inductor was placed in series with a 100 pF capacitor, and the resonant frequency was again measured. After performing this measurement, the coil's inductance could be determined using the resonant frequency, the known capacitance, and equation 9. Once the coil's inductance was known, the chamber's capacitance was determined using equation 9. The vacuum chamber's capacitance is 92 pF.

After determining the chamber's capacitance, a copper inductor coil and variable resistor were added to the circuit. The inductor and cyclotron chamber resonated at 15.1 MHz. The variable capacitor was tuned so that the circuit had an impedance of 50 Ohms. Once the circuit was tuned, it was tested for arcing with 100 W pulses. During testing, the chamber was connected to an oscilloscope that displayed the incident and reflected signal. A chamber that is not arcing produces a signal that is invariant in time. The chamber did not arc during the 100 W pulses.

A circuit's quality factor (Q) is a dimensionless number representing the ratio of the total energy stored in an oscillating system to the energy lost in a single cycle. Q can be represented schematically on a graph of current versus frequency, as shown in Figure 9. Q is defined as the resonant frequency (f_0) of the system divided by the bandwidth (Δf).

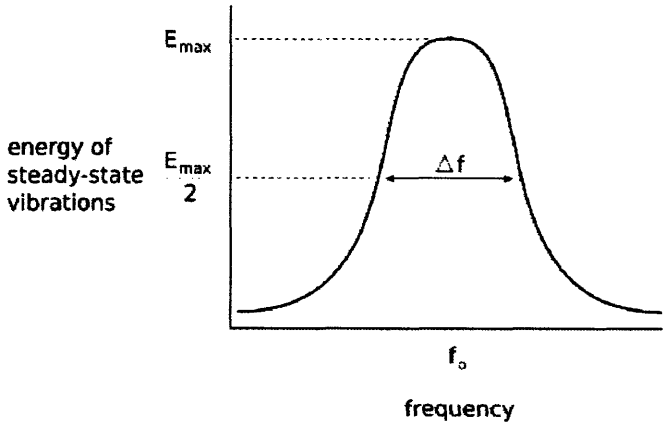

Figure 9. Schematic plot of energy versus frequency for a damped oscillator. Q is defined as $f_0/\Delta f$. (B. Crowell).

Before constructing the cyclotron chamber and electrodes, the Q factor was estimated, using approximations for the system's capacitance and resistance. This estimate is shown in equation 10.

$$Q=\frac{1}{R}\sqrt{\frac{L}{C}} \quad \text{, where R = 4 mOhms} \tag{10a}$$

$$Q=\frac{1}{8.6\cdot 10^{-3}}\sqrt{\frac{190\cdot 10^{-9}}{75*10^{-9}}} = 185 \tag{10b}$$

A more precise value of the Q factor was determined after the chamber and electrodes were built by measuring the bandwidth and resonant frequency of the oscillator. For a resonant frequency of 15 MHz and bandwidth of 80 KHz, Q is equal to 190. This experimentally derived result is gratifyingly similar to the predicted outcome.

Details of Construction

The RF components, shown in Figure 10, are housed in an aluminum box made of bent sheet aluminum. An n-type bulkhead connector mounted directly to the box connects to the function generator and power amplifier that generate the RF signal. The variable capacitor is mounted to the box using Delrin standoffs to prevent arcing. The box also contains a copper inductor coil made of 8 gauge copper wire. The components in the box are connected by 10 gauge copper wire. A copper grounding strap ensured a good electrical connection between the RF source's ground, the RF box, and the vacuum chamber.

Figure 10. Cyclotron RF system in aluminum box with copper grounding strap.

Proton Source

Principles of Operation

The cyclotron's ion source uses electrons to ionize hydrogen gas, thereby generating protons. The electrons are generated by thermionic emission. Thermionic emission occurs when electrons on the surface of a hot conductor (on the order of 1000 – 3000K) have enough kinetic energy to overcome the electrostatic forces binding them to the surface. In this cyclotron's ion source, the electrons flow from a negatively biased neodymium filament to the chamber ground. Figure 11 is a circuit diagram showing the flow of electrons in the ion source. These electrons have sufficient energy to ionize hydrogen gas to form protons.

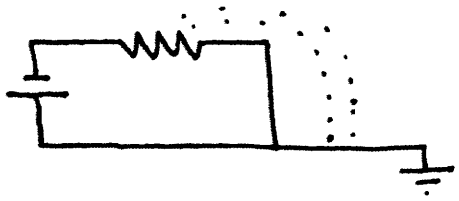

Figure 11. Ion source schematic, indicating electron flow.

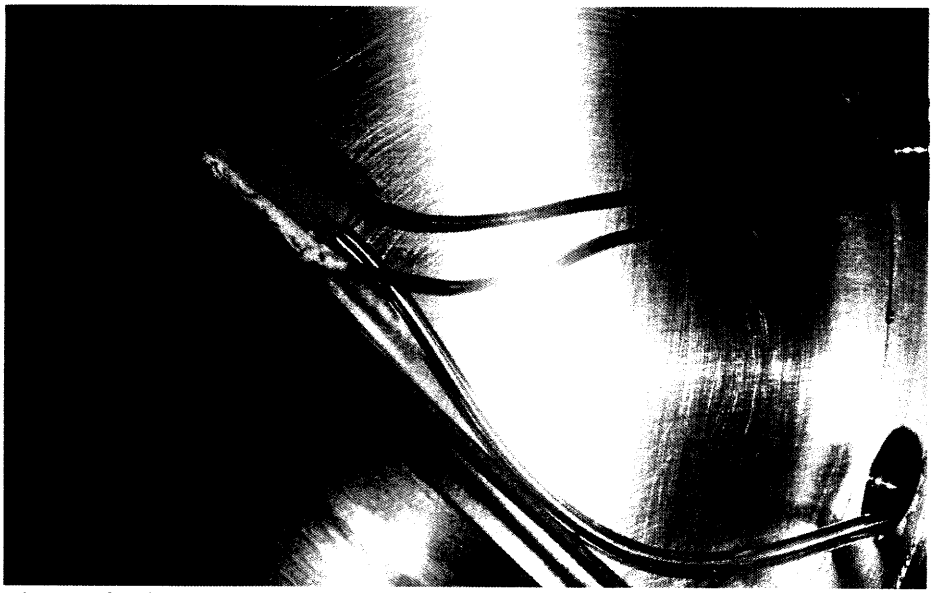

Figure 12. Cyclotron ion source, showing wires connecting to neodymium wire filament and hydrogen inlet tube.

Details of Construction

Figure 12 shows the completed ion source. The filament is made of neodymium wire, which is connected to a vacuum-tight feedthrough (Kurt J. Lesker, part number EFT0024038). There are 22 Ohms of resistance across the feedthrough leads. The filament temperature must be approximately 1000 K for thermionic emission to occur. The wire achieves this temperature when approximately 10 volts are applied across the filament.

Proton Detector

Principles of Operation

The protons were detected at the end of their flight path using a Faraday cup. A copper rod, which was connected to ground through an amplifier (Stanford Research Systems SRS560) was positioned 7.34 cm from the center of the cyclotron chamber. Protons incident upon the copper rod generate a current. The copper rod is shielded with copper flashing to reduce measurement noise.

There are also negative ions in the chamber produced when the hydrogen gas is ionized. These negative ions travel in an opposite direction to the positive protons. If these negative ions strike the copper rod, they will neutralize the protons' signal. Therefore, the copper rod is shielded by a piece of aluminum connected to the chamber ground. Negative particles strike this grounded aluminum, and therefore do not affect the measurement. Figure 13 shows the cyclotron's proton detector.

Figure 13. Proton detector and copper flashing which ensures constant connection to ground and shields detector.

Details of Construction

The detector has a vacuum-tight feedthrough made by press-fitting the copper detector rod through a piece of Delrin, which was in turn press-fit through a length of copper tubing. The copper rod is shielding with copper flashing and an aluminum housing box. A BNC connector, which connects to the amplifier, is mounted to the aluminum housing.

Conclusions and Additional Testing

Figure 14 shows the closed cyclotron chamber, RF box, and mounting plates. I was unable to test the cyclotron's proton source and detector before writing this document, because there was no hydrogen available for the ion source. These components will be tested during the week of May 27, 2007. The modules of the cyclotron that have been tested—the RF system and vacuum chamber—all function successfully. The vacuum chamber can consistently hold a vacuum of approximately $2*10^{-3}$ Torr. The RF system, which has a quality factor of 190, does not arc when subjected to 100 W pulses. Following testing of the remaining two modules, the cyclotron's inductor will be tuned to 160 nH (by equation 9), creating a resonance at 41.2 Mhz (by equation 3). The variable capacitor will then be adjusted to match the incoming signal impedance, and the applied magnetic field will be set to 2.7 Tesla. Adjusting these parameters will make the system capable of producing a beam of 1.88 MeV protons, which will drive the Li7(p, n)Be7 reaction.

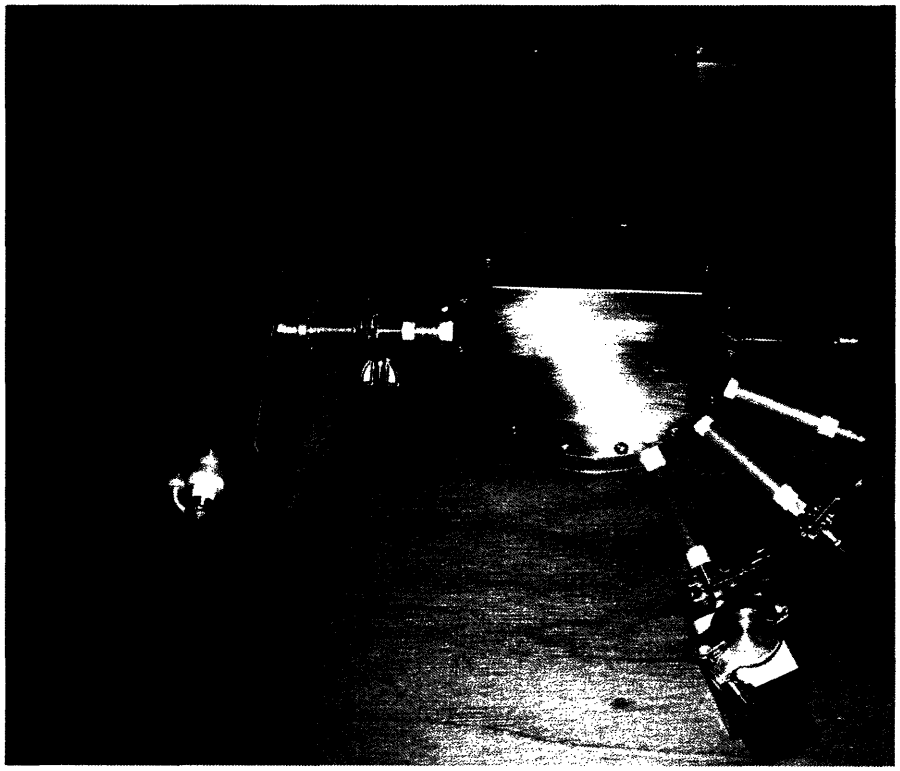

Figure 14. Closed cyclotron chamber, RF box, and mounting plates.

References

[1] Bair, J. "Proton Bombardment of Lithium." Physical Review. 1952.

[2] Bashkin, S. "Proton Bombardment of Lithium Isotopes." Physical Review. 1951.

[3] Bodansky, D. "Neutron Energy Distribution in Proton Bombardment of Beryllium." Physical Review. 1950.

[4] Clegg, A. "Gamma Radiation from the Medium Energy Proton Bombardment of Lithium, Beryllium, Boron, Carbon, and Nitrogen." Proceedings of the Physical Society. 1961.

[5] Hahn, T. "Neutrons and Gamma Rays from the Proton Bombardment of Beryllium." Physical Review. 1952.

[6] Oppenheimer, JR and JS Schwinger. "On Pair Emission in the Proton Bombardment of Fluorine." Physical Review. 1939.

[7] Lawrence, E, and M Livingston. The Production of High Speed Ions Without the Use of High Voltages. 1932.

[8] Livingston, M. Particle Accelerators. Cambridge, Massachusetts: Harvard University Press, 1969.

[9] Machinery's Handbook, 27th Edition. Eds: R Oberg, J Jones, K Horton, R Ryffel, S McCauley, D Heald and O Hussain. New York, New York: Industrial Press, 2004.

[10] Rosenblatt, J. Particle Acceleration. Methuen, 1968.

[11] Rutgers Cyclotron. http://www.physics.rutgers.edu/cyclotron/. Created March 2003, Viewed September 2006.

[12] Scharf, W. Particle Accelerators and Their Uses. Amsterdam: Harwood Academic Publishers, 1986.

[13] Wilson, R., and R Littauer, Accelerators: Machines of Nuclear Physics. New York, New York: Doubleday, 1960.

[14] Young, W., and R Budynas. Roark's Formulas for Stress and Strain, Seventh Edition. New York, New York: McGraw-Hill, 2002.

Appendix A: Proton Flight Path and Mean Free Path Calculations

```
function cyclotron_and_mfp

m = 1.67*10^-27; % mass of proton, kg
q = 1.602*10^-19; % proton charge, C
r_max = 0.076; % maximum proton flight path radius, m

B = 2.5; % magnetic field strength, Tesla
volts = 50; % applied voltage, volts

freq = q*B/(2*pi*m); %cyclotron frequency, Hz

r = 0; % initial proton flight path radius
t = 0; %initializing time variable
i = 1; % initializing index i
delta_t = 10^-7; % time increment, s

while r < r_max % while the proton's flight path radius is less than the dee's
radius
    dEdt = 2*volts*q*freq; % rate of energy input into the cyclotron.

    KE = t.*dEdt; % kinetic energy of the proton.
    % st time = 0, the proton's kinetic energy is 0.  All kinetic energy
    % increase is due to the applied voltage between the dee and dummy dee.

    v = sqrt(2*KE/m); % proton velocity, which is a function of its KE

    r = m*v/(q*B);
    % the radius of the proton's flight path is a function of it's KE, and
    % is therefore a function of its velocity

    t = t + delta_t; % increment time

    % store the following in vectors, to be read later:
    time(i) = t;
    kineticenergy(i) = KE/(1.6*10^-13);
    velocity(i) = v;
    radius(i) = r;
    flightdistance(i) = v*delta_t;

    i = i+1; %increment index
end

KE_max = max(kineticenergy)

totalflight = sum(flightdistance) %determine the proton's total flight path

%plot(time,velocity,'*')
```

```
%ts = timeseries

x = radius.*sin(2*pi.*time*freq);
y = radius.*cos(2*pi.*time*freq);
%plot(x,y,'.')

%estimating mean free path
r_proton = .8*10^-15;
r_oxygen = 2*60*10^-12;
r_nitrogen = 150*10^-12;

r_ave = 10^-12;

P = [0.001 0.01 0.1 1 10 100]; %pressure, Pa
RB = 8.31; %universal gas constant
T = 300; %temperature in Kelvin

NA = 6.022*10^23;

molardensity = P/(RB*T);
moleculardensity = NA*molardensity;
mfp = 1./(pi*r_ave^2*moleculardensity)

pascal_to_torr = 0.0075

x = 0.0001:0.001:10;
loglog(P*pascal_to_torr, mfp, x, 7*10^3)
title('Proton Mean Free Path vs Vacuum Pressure')
xlabel('Pressure, Torr')
ylabel('Mean Free Path, m')
%flight_to_mfp_ratio = totalflight/mfp
```